JOURNAL OF COMPUTATIONAL PHYSICS **132,** 3–11 (1997)
ARTICLE NO. CP965514

A Well-Behaved TVD Limiter for High-Resolution Calculations of Unsteady Flow

Mohit Arora and Philip L. Roe

Department of Aerospace Engineering, University of Michigan, Ann Arbor, Michigan 48109-2118

Received October 16, 1995; revised May 13, 1996

A total variation diminishing (TVD) limiter is proposed that attempts to maximize performance given that the inherent limitation of TVD formulations is peak loss. For the scalar advection and Burger's equation, the present results are qualitatively superior to those using the harmonic and superbee limiters, balancing well the competing effects of skewing, smearing, and squaring. In the case of the Euler equations, the current results appear to significantly improve upon previous TVD results and are quite comparable with more elaborate algorithms. © 1997 Academic Press

1. INTRODUCTION

Control of oscillations in high-resolution schemes continues to be a topic of interest and importance. Many methods are based on Harten's concept of a total variation diminishing (TVD) scheme, which prevents, in the scalar case, any values being generated after $n + 1$ time steps that lie outside the range of those present after n time steps. There are several other properties that are loosely equivalent—positivity [21], the characteristic interpolation property [15], or local extremum diminishing [7]. If any of these conditions apply, then the amplitude of any genuine extremum can only decrease, and there is a progressive loss of information concerning high-frequency waves.

To remedy this, Harten *et al.* [4, 5] introduced the idea of essentially nonoscillatory (ENO) schemes, which allow the loss of amplitude at one step to be regained at another. Numerous comparison studies show that ENO schemes preserve the high-frequency information better than TVD schemes. Usually, however, the comparison is made with an inferior TVD method.

This seems to have an historical origin. Early studies of flux-limiter schemes [13, 16, 17, 22] were based on unsteady analysis of the advection equation and retained the Courant number $\nu = a\,\Delta t/\Delta x$ as a parameter in the analysis, leading to constraints (the notation is defined later)

$$\Phi(r) \le \min\left(\frac{2}{1-\nu}, \frac{2r}{\nu}\right).$$

For the most part, the analysis was subsequently applied to finding steady solutions as the large-time limit of a (pseudo) unsteady flow. Retaining the dependence on the Courant number shows little advantage in these circumstances, and the simplified condition

$$\Phi(r) \le \min(2, 2r)$$

is more economical. Additionally, if the limiter has the symmetry property

$$\Phi\left(\frac{1}{r}\right) = \frac{1}{r}\,\Phi(r),$$

then simplified reconstruction techniques [23] can be used that reduce the computational cost.

These simplifications do, however, reduce the effectiveness of TVD schemes in their original setting of unsteady flow, and it is these simplified schemes that have usually been compared with ENO schemes, much to the advantage of the latter. The object of the present paper is to point out that TVD schemes, as originally conceived, are not in fact inferior to the simpler kinds of ENO schemes and can be substantially cheaper. We do not wish to over-sell the product and readily concede that elaborate ENO schemes can give superior performance. We do, however, wish to correct the impression that TVD schemes are without merit for unsteady flow.

The cost of the proposed limiter is one call each to the max and min functions, the same as for the minmod limiter. This limiter is now new [12, 16] and has recently been suggested by Jeng and Payne [8] as a basis for an adaptive limiter with shock-detection features. Neither is it perfect; there is a limit (pun intended) to what can be accomplished with the fixed stencil of a TVD scheme. Having said that, it *does* perform much better than the TVD schemes presently in common use.

2. DESIGNING THE LIMITER

Ideally, a limiter should possess the following properties:

0021-9991/97 $25.00

1. be a homogeneous function
2. satisfy the TVD constraints
3. be as accurate as possible in smooth regions
4. revert to the underlying first-order scheme at extrema and discontinuities
5. be computationally simple and economical
6. convert smooth profiles without undue distortion
7. convect discontinuities without much smearing
8. accomplish all of the above for a wide range of Courant numbers.

To be successful at all Courant numbers, it is highly probable that some dependence on this parameter must be retained. The behavior of the superbee limiter near the point (1, 1) is designed [13] to bestow a discontinuity-capturing property for linear waves. It has proved difficult to retain this without also having to accept a tendency to "square off" smooth profiles, but if this is tolerable, superbee remains a good choice. An alternative criterion for the behavior near (1, 1), also noted in [13], is to choose the unique slope at that point that gives third-order accuracy in the one-dimensional constant coefficient case. This leads to a class of limiters given by

$$\Phi(s_1, s_2, \Phi_{\max}, r) = \max[0, \min\{s_1 r, 1 + s_2(r - 1), \Phi_{\max}\}].$$

This function is made up of three straight-line segments, two of which are fully determined by the TVD constraints, i.e., $s_1 = 2/\nu$ and $\Phi_{\max} = 2/(1 - \nu)$. The segment that remains to be determined is the middle one. Observe that it must pass through the point (1, 1) in order to revert to the second-order scheme in smooth regions. We choose s_2 to be the slope corresponding to the third order scheme at the point (1, 1) in (r, Φ) coordinates, viz.,

$$s_2 = \left(\frac{1 + \nu}{3}\right), \tag{2.1}$$

which fully determines the proposed limiter function. This limiter function was used by Roe and Baines [12, 16] almost 15 years ago. More recently, this function was utilized by Jeng and Payne [8] in the context of an adaptive limiter; because of the stress placed on discontinuity capturing in [8], the authors perhaps undervalued it as a general-purpose limiter. Although TVD schemes in general cannot be better than second-order accurate, this particular limiter bestows some properties characteristic of third-order schemes. Experiments reported in [12] demonstrated that for linear advection the width of a discontinuity in the initial data spreads like $t^{1/4}$, rather than the $t^{1/3}$ typical of second-order methods. This is reflected in the excellent resolution of contact discontinuities in the results below.

Note that the stability restriction on the method is simply $|\nu| \le 1.0$.

For non-linear systems, the full TVD region has been empirically found to be too compressive and hence we use the more restrictive TVD constraints of $s_1 = \Phi_{\max} = 2$ for the nonlinear waves while using the full TVD region for the linear waves. This bound could probably be relaxed for problems involving only weak shocks. This is analogous to the popular implementation of using the harmonic limiter on the non-linear waves and the Superbee limiter on the linear waves. Researchers who follow this practice might find that the present limiter would also be an appropriate choice for the linear fields.

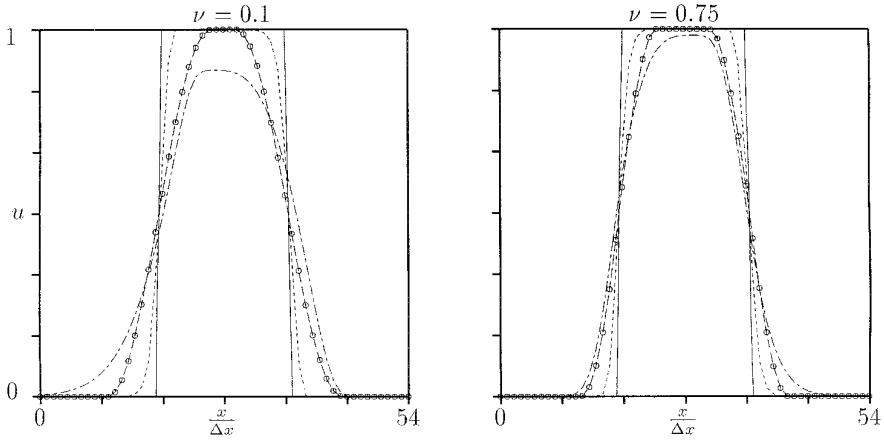

FIG. 1. Solution to the scalar advection equation for a square wave: $u_0 = 1$ if $(a + 1) \le x/\Delta x \le (b - 1)$ ($u_0 = 0$ otherwise) where $b - a = 20$ [exact (solid line), harmonic limiter (–––), superbee limiter (---), and the proposed limiter (o)]. Left-hand figure: $t = 9$, $\nu = 0.1$, 9000 time steps. Right-hand figure: $t = 9$, $\nu = 0.75$, 1200 time steps.

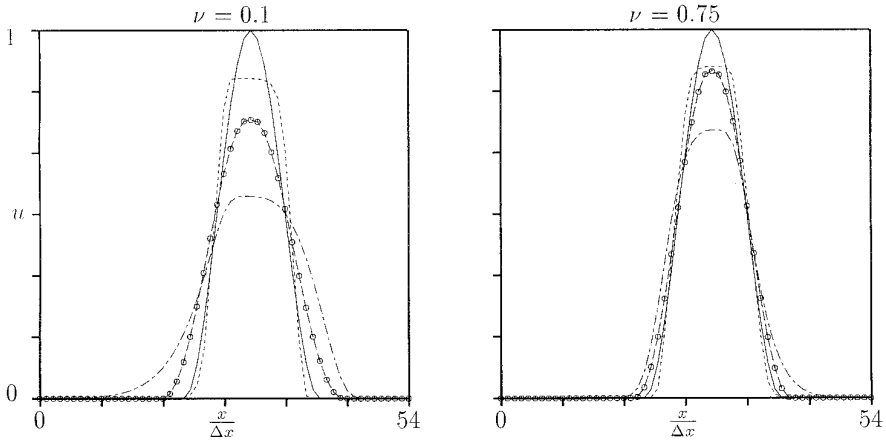

FIG. 2. Solution to the scalar advection equation for a $\sin^2 x$ wave $u_0 = \sin^2[\pi(x/\Delta x - a)/(b - a)]$ if $a \le x/\Delta x \le b$ ($u_0 = 0$ otherwise) where $b - a = 20$ [exact (solid line), harmonic limiter (–––), superbee limiter (---), and the proposed limiter (o)]. Left-hand figure: $t = 9$, $\nu = 0.1$, 9000 time steps. Right-hand figure: $t = 9$, $\nu = 0.75$, 1200 time steps.

3. SOME REMARKS ON IMPLEMENTATION

We write the flux at the interface between cells j and $j + 1$, in terms of the eigenvalues and eigenvectors of the Roe-averaged matrix [14], as

$$F_{j+1/2} = \frac{1}{2}[F_j + F_{j+1}] - \frac{1}{2}\sum \alpha_k|\lambda_k|\mathrm{r}_k + \frac{1}{2}\sum \Phi_k(1 - |\nu_k|)\alpha_k|\lambda_k|\mathrm{r}_k, \tag{3.1}$$

where the first term is a symmetric (central) flux, the second term gives the basic upwind scheme, and the third term can be thought of as an anti-diffusive flux, depending on the limiters Φ_k. Setting these to unity gives the Lax–Wendroff scheme. For linear problems on uniform grids the input to the limiter is the ratio of the upwind to central slopes in the data,

$$r^+_{j+1/2} = \frac{\Delta u_{j-1/2}}{\Delta u_{j+1/2}},$$

$$r^-_{j+1/2} = \frac{\Delta u_{j+3/2}}{\Delta u_{j+1/2}},$$

where r^+ is to be used if the wave is right-moving (between j, $j + 1$), otherwise r^- is used.

Limiting based on the reconstruction of characteristic

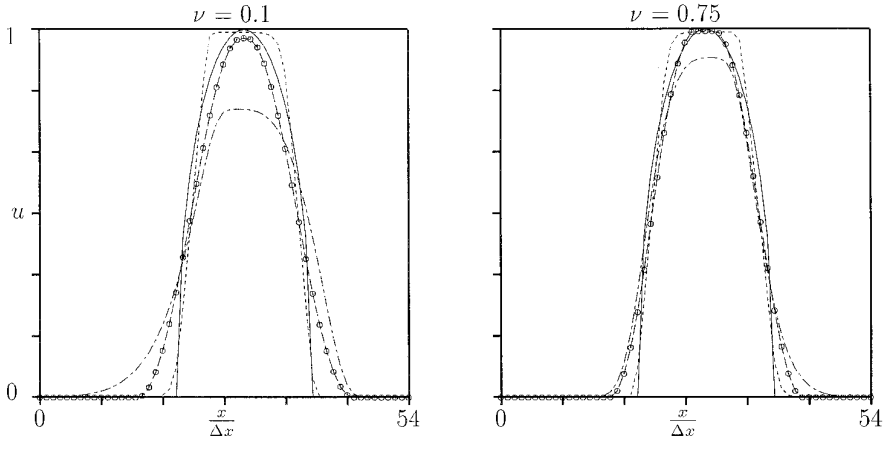

FIG. 3. Solution to the scalar advection equation for a half-ellipse wave $u_0 = [1 - 4\{(x/\Delta x - (a + b)/2)/(b - a)\}^2]^{1/2}$ if $a \le x/\Delta x \le b$ ($u_0 = 0$ otherwise) where $b - a = 20$ [exact (solid line), harmonic limiter (–––), superbee limiter (---), and the proposed limiter (o)]. Left-hand figure: $t = 9$, $\nu = 0.1$, 9000 time steps. Right-hand figure: $t = 9$, $\nu = 0.75$, 1200 time steps.

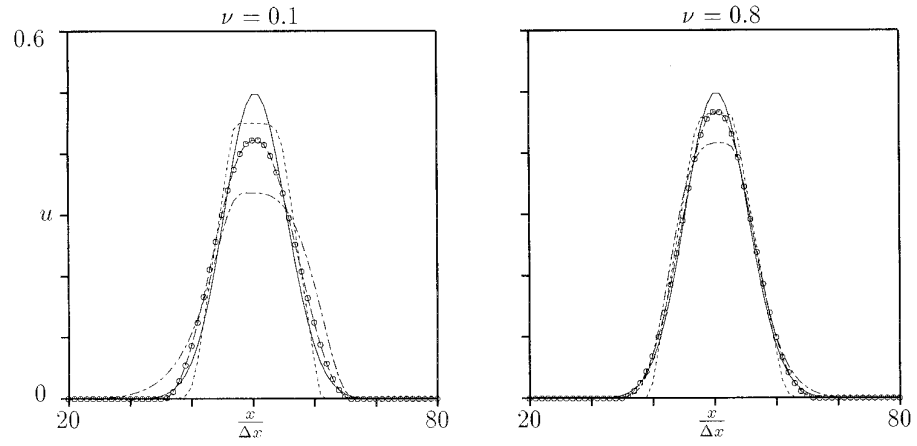

FIG. 4. Solution to the scalar advection equation for the aeroacoustic benchmark $u_0 = \frac{1}{2}\exp[-\log(2)\cdot(x/3)^2]$ $0 \le x \le 100$ [exact (solid line), harmonic limiter (–––), superbee limiter (---), and the proposed limiter (o)]. Left-hand figure: $t = 400$, $\nu = 0.1$, 8000 time steps. Right-hand figure: $t = 400$, $\nu = 0.8$, 1000 time steps.

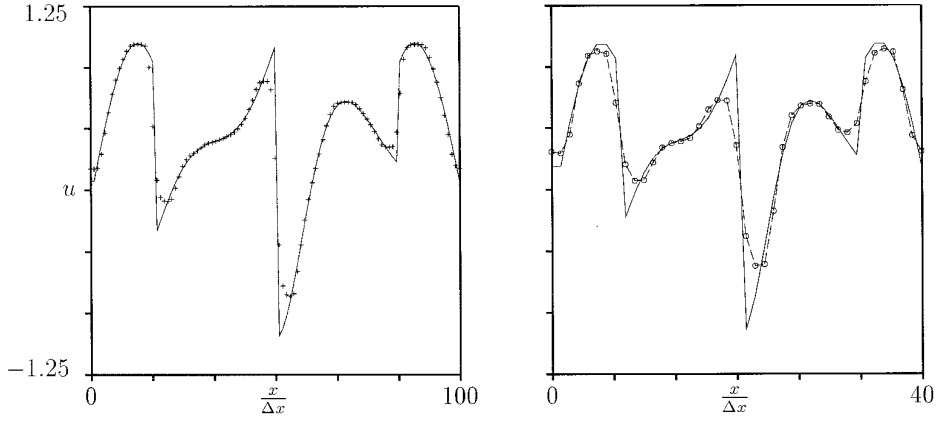

FIG. 5. Solution to the scalar advection equation for Harten's function [3]. Left-hand figure: exact (solid line), superbee limiter (+), $\nu = 0.8$, $t = 2$, 100 cells, 125 time steps (compare to results in [8]). Right-hand figure: exact (solid line), superbee limiter (o), $\nu = 0.8$, $t = 1$, 40 cells, 50 time steps.

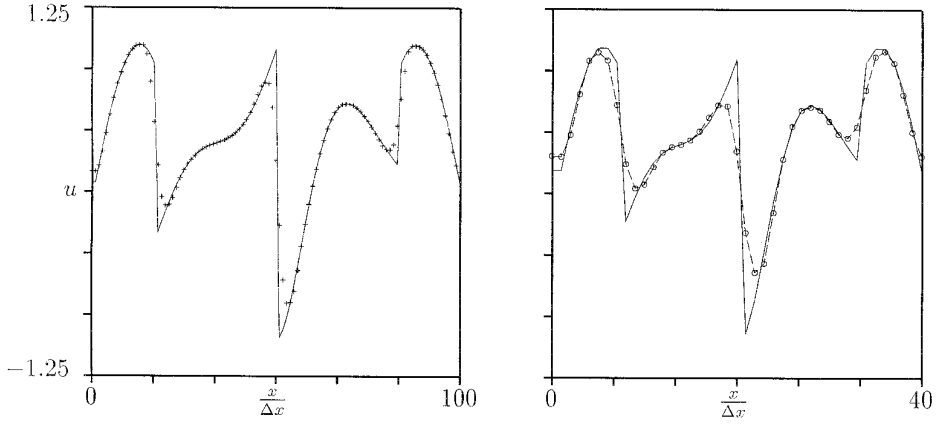

FIG. 6. Solution to the scalar advection equation for Harten's function [3]. Left-hand figure: exact (solid line), present limiter (+), $\nu = 0.8$, $t = 2$, 100 cells, 125 time steps (compare to results in [8]). Right-hand figure: exact (solid line), present limiter (o), $\nu = 0.8$, $t = 1$, 40 cells, 50 time steps.

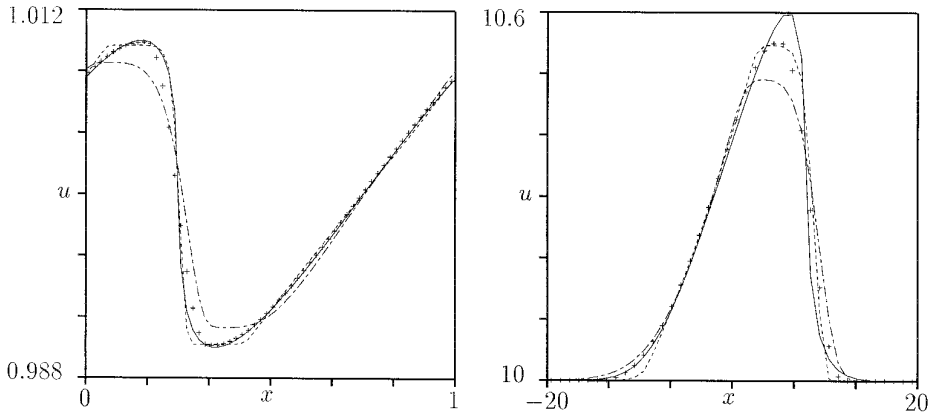

FIG. 7. Solution to Burger's equation for two weakly nonlinear test functions [exact (solid line), harmonic limiter (–––), superbee limiter (---), and the proposed limiter (+)]. Left-hand figure: $u_0 = 1 + 0.01\cos(2\pi x)$, $x \in [0, 1]$, $t = 15$, ν 0.1, 60 cells ($\Delta x = 1/60$), after approximately 9000 time steps (compare to results in [11]). Right-hand figure: $u_0 = 10 + 0.6\exp[-\log(2)\cdot(x/5)^2]$, $x \in [-50, 50]$, $t = 10$, $\nu = 0.1$, 100 cells ($\Delta x = 1$), after approximately 1100 time steps. Only the part of the solution close to the disturbance is shown.

variables would take the input as the ratio of wavestrengths α. Here, we take

$$r^+_{j+1/2,k} = \frac{((1 - |\nu_k|)\nu_k\alpha_k)_{j-1/2}}{((1 - |\nu_k|)\nu_{k\alpha_k})_{j+1/2}},$$

$$r^-_{j+1/2,k} = \frac{((1 - |\nu_k|)\nu_k\alpha_k)_{j+3/2}}{((1 - |\nu_k|)\nu_k\alpha_k)_{j+1/2}}.$$

These definitions are suggested by a nonlinear scalar analysis [13, 22] and we find that they give minor but noticeable improvement over the simpler definitions.

In numerical tests with the Euler equations, a modified time-step

$$\Delta t^* = \Delta t[1 - 0.01(10 - n)^2], \qquad n \le 9,$$

was used, as suggested by Huynh [6]. The reasoning is that, for all self-similar problems, the time step should be constant. However, the first few time steps based purely on the CFL condition turn out to be too large, leading to large "starting errors." This modification to the time step for the first nine steps was shown by Huynh to minimize this problem.

4. NUMERICAL EXPERIMENTS

4.1. *Scalar Advection*

$$u_t + u_x = 0, \qquad u(t = 0) = u_0.$$

The boundaries are periodic. We compare solutions for the harmonic and superbee limiters to those of the proposed limiter for a square wave (Fig. 1), a $\sin^2 x$ wave (Fig. 2), a

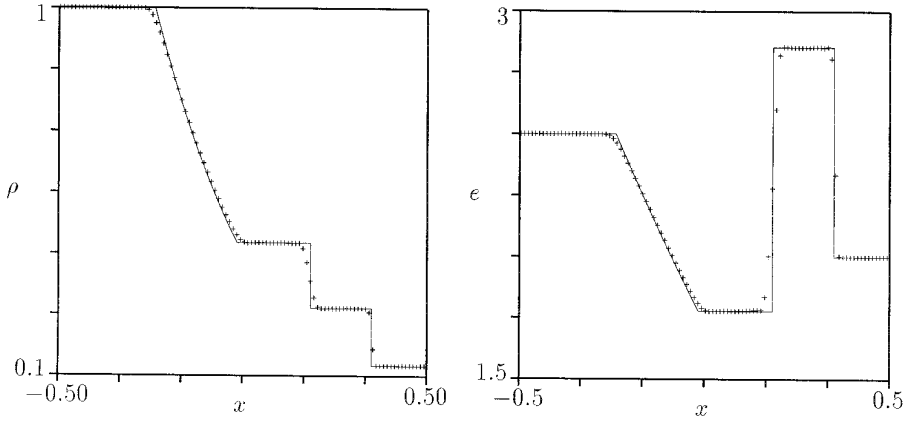

FIG. 8. Solution to the full Euler equations for the Sod test case. We plot density (left) and internal energy (right) [exact (solid line), proposed limiter (+)], $\mathbf{w}_L = (\rho, u, p)^T = (1, 0, 1)^T$, $\mathbf{w}_R = (\rho, u, p)^T = (0.125, 0, 0.1)^T$, $t = 0.2$, $\Delta x = 0.01$ (100 cells), $\nu = 0.8$ (compare to results in [8]).

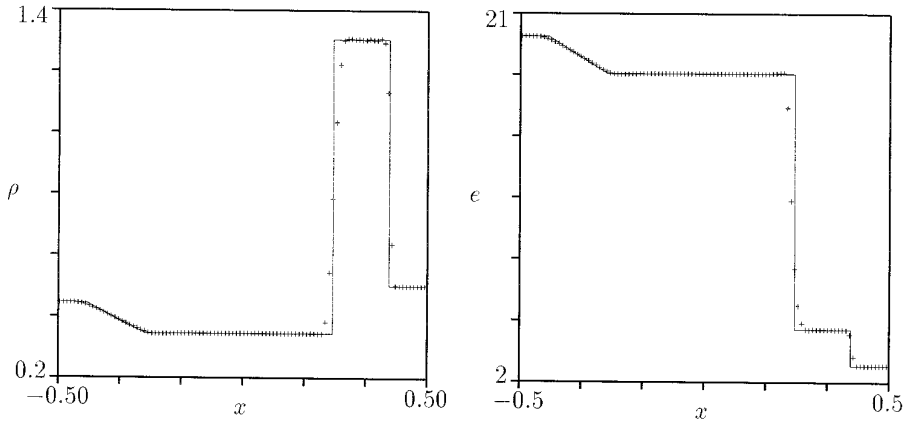

FIG. 9. Solution to the full Euler equations for the Lax test case. We plot density (left) and internal energy (right) [exact (solid line), proposed limiter (+)], $\mathbf{w}_L = (\rho, u, p)^T = (0.445, 0.698, 3.528)^T$, $\mathbf{w}_R = (\rho, u, p)^T = (0.5, 0, 0.571)^T$, $t = 0.16$, $\Delta x = 0.01$ (100 cells), $\nu = 0.8$ (compare to results in [6]).

half-ellipse wave (Fig. 3), and a standard test case for aeroacoustics [2] (Fig. 4). Finally, we compare the superbee limiter (Fig. 5) to the proposed one (Fig. 6) on Harten's test function [3]

$$u_0 = \begin{cases} -x \sin(\frac{3}{2}\pi x^2) & -1 \le x < -\frac{1}{3} \\ |\sin(2\pi x)| & |x| < \frac{1}{3} \\ 2x - 1 - \frac{1}{6}\sin(3\pi x) & \frac{1}{3} < x < 1. \end{cases}$$

4.2. *Burger's Equation*

$$u_t + [u^2/2]_x = 0, \qquad u(t = 0) = u_0.$$

The boundaries are periodic. We compare the harmonic, superbee, and proposed limiters for two weakly nonlinear test cases (Fig. 7). Note that the results for both cases are presented just prior to shock formation to provide a worst case scenario (once the shock forms, the peak losses are swept into the shock and schemes appear better than they really are).

4.3. *The Euler Equations*

$$\mathbf{w}_t + \mathbf{f}_x = 0,$$

$$\mathbf{w}(t = 0) = \mathbf{w}_0 = \begin{cases} \mathbf{w}_L & x < 0 \\ \mathbf{w}_R & x > 0 \end{cases}$$

$$\mathbf{w} = (\rho, \rho u, \rho E)^T, \qquad E = e + \frac{u^2}{2}$$

$$\mathbf{f} = (\rho u, \rho u^2 + p, \rho u H)^T, \quad p = (\gamma - 1)\rho e$$

$$\gamma = \frac{c_p}{c_v} = 1.4.$$

We use absorbing boundary conditions and the results are

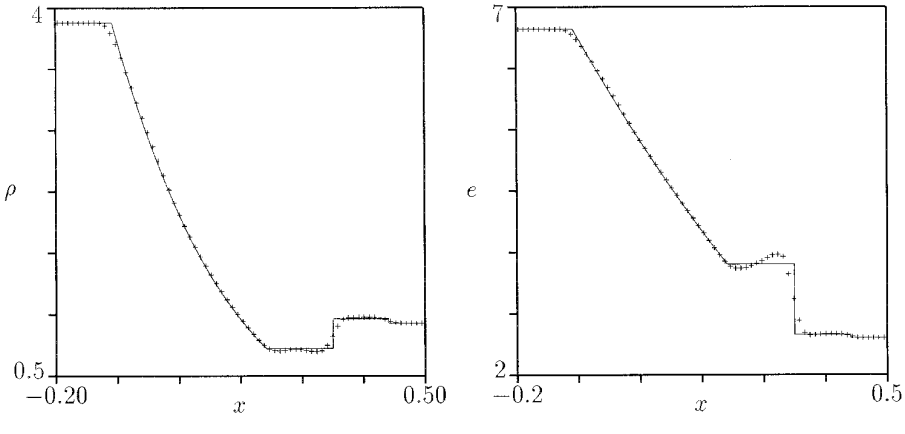

FIG. 10. Solution to the full Euler equations for the Mach 3 test case. We plot density (left) and internal energy (right) [exact (solid line), proposed limiter (+)], $\mathbf{w}_L = (\rho, u, p)^T = (3.857, 0.92, 10.333)^T$, $\mathbf{w}_R = (\rho, u, p)^T = (1, 3.55, 1)^T$, $t = 0.09$, $\Delta x = 0.01$ (100 cells), $\nu = 0.8$ (compare to results in [6]).

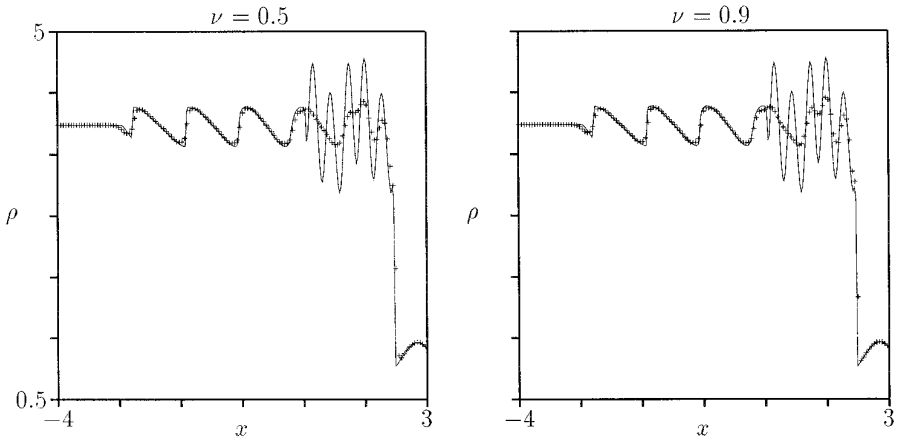

FIG. 11. Solution to the full Euler equations for the Shu–Osher test case. We plot density [exact (solid line), proposed limiter (+)], $\mathbf{w}_L = (\rho, u, p)^T = (3.857, 2.629, 10.333)^T$, $\mathbf{w}_R = (\rho, u, p)^T = [1 + 0.2 \sin(5x), 0, 1]^T$, $t = 1.8$, $\Delta x = 0.05$ (200 cells), $\nu = 0.5$ (left) and 0.9 (right) (compare to results in [1]).

shown for the proposed limiter with restrictive limits of $s_1 = 2 = \Phi_{\max}$ on the nonlinear waves and the full TVD limit on the linear waves. Benchmark results are presented for the Sod (Fig. 8), Lax (Fig. 9) and Mach 3 rarefaction (Fig. 10) cases. The results in Figs. 8, 9 appear to be a little cleaner than those in [10], especially at the contact, and these in turn are generally better than the second- and even fourth-order results in [4].

Finally, we show three sets of results for the Shu–Osher case [20] (Figs. 11–13). We require 800 points to produce a convincing solution to this problem, whereas a (much more elaborate) ENO scheme can do about as well with only 400 points [18]. Jiang and Shu [9] have recently suggested that the quality of the transmitted entropy wave is a good measure of fidelity for the solution of this problem. They show (with slightly modified problem parameters) excellent agreement with the transmission coefficient predicted by small disturbance theory and negligible attentuation of the transmitted wave, using about 20 grid points per wavelength. We get similar quality with about 40 points per wavelength, whereas [9] shows significant attenuation from a ''typical second-order scheme'' [10] using 50 points per wavelength. This places our scheme about halfway between ''typical second-order schemes'' and ''elaborate ENO schemes,'' a placing with which we feel comfortable.

5. DISCUSSION AND CONCLUSIONS

A natural consequence of using a TVD formulation is some peak loss and flattening of profiles. This work at-

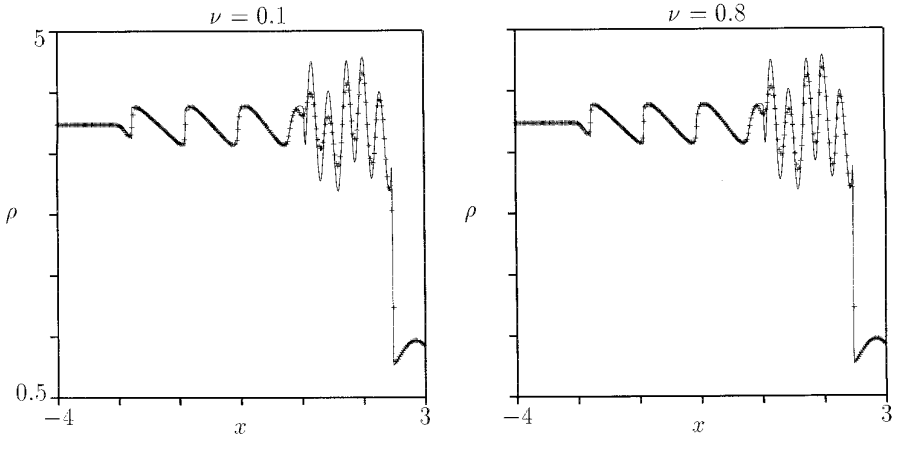

FIG. 12. Solution to the full Euler equations for the Shu–Osher test case. We plot density [exact (solid line), proposed limiter (+)], $\mathbf{w}_L = (\rho, u, p)^T = (3.857, 2.629, 10.333)^T$, $\mathbf{w}_R = (\rho, u, p)^T = [1 + 0.2 \sin(5x), 0, 1]^T$, $t = 1.8$, $\Delta x = 0.025$ (400 cells), $\nu = 0.1$ (left) and 0.8 (right) (compare to results in [11]).

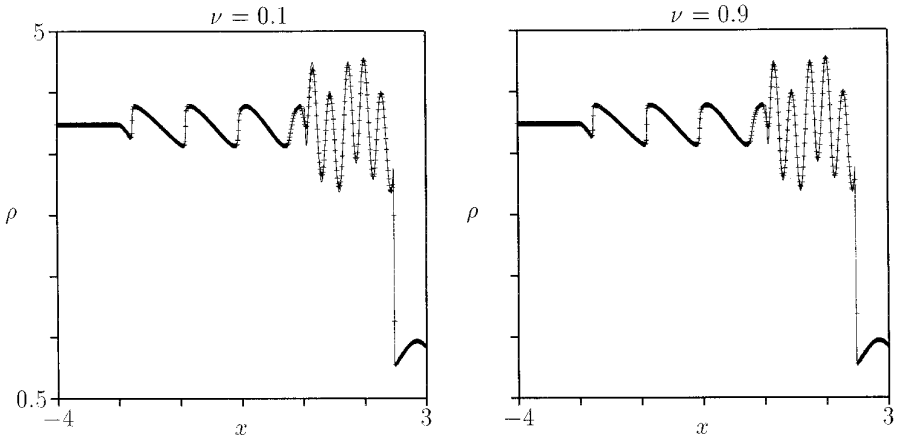

FIG. 13. Solution to the full Euler equations for the Shu–Osher test case. We plot density [exact (solid line), proposed limiter (+)], $\mathbf{w}_L = (\rho, u, p)^T = (3.857, 2.629, 10.333)^T$, $\mathbf{w}_R = (\rho, u, p)^T = [1 + 0.2 \sin(5x), 0, 1]^T$, $t = 1.8$, $\Delta x = 0.0125$ (800 cells), $\nu = 0.1$ (left) and 0.9 (right) (compare to results in [11]).

tempts to maximize performance given these inherent limitations.

From the results presented for scalar advection and Burger's equation, it is clear that the proposed limiter is better qualitatively than the harmonic and superbee limiters (except for the square wave, where superbee is preferable). It has superior shape-preservation properties across a wide range of Courant numbers, and appears to be a good compromise between the competing effects of skewing, smearing and squaring. Further, the results for the Euler equations demonstrate that the limiter proposed here is a significant improvement over previous results for TVD schemes (including those shown in [8]), and is quite competitive with the simpler ENO schemes [1]. Further, our results are almost as good as those obtained by far more elaborate algorithms [11, 6]. Taking into account the fact that this function costs only as much as the minmod limiter and does not expand the computational stencil, it becomes an attractive candidate and can easily be incorporated into existing codes. Note that TVD schemes are more economical than ENO schemes, including efficient implementations of ENO schemes [19, 20]: lower computational cost (smaller number of operations as well as absence of optimal stencil searches and related logic), less restrictive time-steps and lower storage requirements. Finally, the results presented here provide a convenient set of (more accurate) TVD benchmark test cases for researchers to compare their results against.

REFERENCES

1. R. Hannappel, T. Hauser, and R. Friedrich, A comparison of ENO and TVD schemes for the computation of shock-turbulence interaction, *J. Comput. Phys.* **121,** 176 (1995).
2. J. C. Hardin, J. R. Ristorcelli, and C. K. W. Tam (Eds.), ICASE/LaRC Workshop on Benchmark Problems in Computational Aeroacoustics (CAA), NASA Conference Publication 3300, 1995.
3. A. Harten, High-resolution schemes for hyperbolic conservation laws, *J. Comput. Phys.* **49** (1983), 357–393.
4. A. Harten, B. Enquist, S. Osher, and S. R. Chakravarthy, Uniformly high order accurate essentially non-oscillatory schemes, III, *J. Comput. Phys.* **71** (1987), 231–303.
5. A. Harten and S. Osher, Uniformly high-order accurate nonoscillatory schemes, I, *SIAM J. Numer. Anal.* **24,** 279 (1987).
6. H. T. Huynh, Accurate upwind methods for the Euler equations, NASA Tech. Rep. TM 106388 (NASA Lewis Research Center, 1993).
7. A. Jameson, Analysis and design of numerical schemes for gas dynamics, 1. Artificial diffusion, upwind biasing, limiters and their effect on accuracy and multigrid convergence, *Int. J. Comput. Fluid Dynamics,* to appear (1995).
8. Y. N. Jeng and U. J. Payne, An adaptive TVD limiter, *J. Comput. Phys.* **118** (1995), 229–241.
9. G.-S. Jiang and C.-W. Shu, Efficient implementation of weighted ENO schemes, Tech. Rep. 95-73, (ICASE, 1995).
10. X.-D. Liu and P. Lax, Positive schemes for solving multi-dimensional hyperbolic systems of conservation laws, CFD Rev., to appear.
11. R. B. Lowrie, P. L. Roe, and B. van Leer, A space-time Discontinuous Galerkin method for the time-accurate numerical solution of hyperbolic conservation laws, extended abstract submitted to the *12th AIAA CFD Conference, 1995.*
12. P. L. Roe, Numerical algorithms for the linear wave equation, Tech. Rep. 81047 (Royal Aircraft Establishment, 1981).
13. P. L. Roe, Some contributions to the modelling of discontinuous flows, in *Large-Scale Computations in Fluid Mechanics,* Lectures in Applied Mathematics, Vol. 22 (Springer-Verlag, New York/Berlin, 1985), p. 163.
14. R. L. Roe, Characteristic-based schemes for the Euler equations, *Ann. Rev. Fluid Mech.* **18,** 337 (1986).
15. P. L. Roe, A survey of upwind differencing techniques (invited lecture) in *Eleventh International Conference on Numerical Methods in Fluid Dynamics,* Lecture Notes in Physics, Vol. 323 edited by D. L,

Dwoyer, M. Y, Hussaini, and R. G. Voigt, (Springer-Verlag, New York/Berlin, 1988), p. 69.

16. P. L. Roe and M. J. Baines, Algorithms for advection and shock problems, in *Proceedings of the Fourth GAMM Conference on Numerical Methods in Fluid Mechanics,* Notes on Numerical Fluid Mechanics, Vol. 5, edited by H. Viviand (Vieweg, 1981), p. 281.
17. P. L. Roe and M. J. Baines, Asymptotic behaviour of some non-linear schemes for linear advection, in *Proceedings of the Fifth GAMM Conference on Numerical Methods in Fluid Mechanics,* Notes on Numerical Fluid Mechanics, Vol. 7, edited by M. Pandolfi and R. Piva (Vieweg, 1983), p. 283.
18. C.-W. Shu, Numerical experiments on the accuracy of ENO and modified ENO schemes, *J. Sci. Comp.* **5,** 127 (1990).
19. C.-W. Shu and S. Osher, Efficient implementation of essentially non-oscillatory shock-capturing schemes, *J. Comput. Phys.* **77,** 439 (1988).
20. C.-W. Shu and S. Osher, Efficient implementation of essentially non-oscillatory shock-capturing schemes, II, *J. Comput. Phys.* **83,** 32 (1989).
21. S. P. Spekreijse, Multigrid solution of monotone second-order discretizations of hyperbolic conservation laws, *Math. Comput.* **49,** 135 (1987).
22. P. K. Sweby, High resolution schemes using flux limiters for hyperbolic conservation laws, *SIAM J. Numer. Anal.* **21,** 995 (1984).
23. B. Van Leer, Towards the ultimate conservative difference scheme. V. A. second-order sequel to Godunov's method, *J. Comput. Phys.* **32,** (1979).